The 18th IEEE International Symposium on
Robot and Human Interactive Communication
Toyama, Japan, Sept. 27-Oct. 2, 2009

Adaptive CPG Based Coordinated Control of Healthy and Robotic Lower Limb Movements

Jae-Kwan Ryu, Nak Young Chong, Bum Jae You, and Henrik Christensen

Abstract— **This paper proposes an adaptive CPG based controller for a lower limb prosthesis consisting of online trajectory generation and interlimb coordination. The adaptive CPG can produce multidimensional rhythmic patterns and modulate their frequency by tuning relevant parameters in an autonomously way adapting to a changing periodicity of external signals. Also, to increase the stability of the prosthesis, a spring-damper component is attached between the hip and ankle joints, allowing the absorption of impulsive ground reaction forces at landing. We verify the validity of the proposed controller with a simulated humanoid robot through the investigation of the self-coordination between the healthy and robotic legs.**

I. INTRODUCTION

In recent years, there has been increasing attention paid to robotic rehabilitation such as limb prostheses and exoskeletons. Particularly, a lower limb prosthesis is not only important to the functional replacement for an amputated limb, but also help to restore the dignity of amputees [1]. In this paper, we take inspiration from biology to design a highly functional prosthesis. Humans and animals are able to learn and perform skilled movements adapting to changing conditions quickly and easily. Many researchers used signals from the human brain to control artificial limb motions [2], [3], [4]. Likewise, central pattern generators (CPGs) with coupled neural oscillators appear to be effective in controlling locomotion [5], [6], [7] and repetitive arm movements [8]. Notably, a 2D biped was simulated under unpredicted conditions using neural oscillators in [5].

Toward the application of biologically inspired robotics to lower limb rehabilitation, this work investigates the usefulness of a network of neural oscillators, particularly in achieving automatic coordination between the healthy and robotic lower limbs. Neural oscillators synchronize or lock onto the input signal, and adapt themselves to the dynamics of the coupled system. However, it is usually difficult to tune the parameters of an oscillator to ensure that the oscillator synchronizes to a variety of input signals [9], [10], [11], [12]. For instance, if the frequency of the input signal is far away from the oscillators' intrinsic frequency, the synchronization between those frequencies will not occur and also the oscillator's output pattern will not be maintained. Therefore, the parameters that are related to the frequency of the oscillator need to be adjusted in accordance with the changes in the input signal frequency. Such a modulation will enhance the robustness of the oscillator and facilitate easy determination of parameters for the desired oscillator signal. Several techniques have been proposed for designing adaptive oscillators that can lock onto a wider range of time-varying input signals. Most existing techniques are based on various learning models [12], [13], [14], a learning rule [9], and an observer-based method [10].

Our primary concern in this work is how to maintain synchronization between the healthy and robotic lower limbs. Specifically, we propose an adaptive CPG based swing frequency controller for a robotic lower limb that can automatically adapt to a changing landing periodicity of the healthy leg. The adaptive CPG can continuously produce a coordinated multidimensional rhythmic pattern and modulate its frequency by self-tuning the relevant parameters adapting to a variety of input signals. In addition, a spring-damper component is attached between the hip and ankle joints to absorb the impulsive ground reaction force at landing, enabling to cope with a lack of structural compliance of the robotic lower limb. We verify the validity of the proposed adaptive control architecture using a simulated humanoid robot HOAP-3.

II. FREQUENCY-ADAPTIVE OSCILLATOR

We present our evolutionary computation method to design a rule for adapting nonlinear oscillators to varying input signals and adaptive sensory motor functions for lower limb coordination. To the best of our knowledge, no previous evolutionary method for the frequency-adaptive rule of neural oscillators can be found in the literature.

1) Neural Oscillator: For realizing the adaptive CPG, we use Matsuoka's neural oscillator model [18]. This model is a half-center oscillator consisting of two neurons having mutually inhibitory interactions. It has been widely applied in robotics over the past several decades [5], [6], [8], [19]. The model can be described by the following set of differential equations:

$$\tau_1 \dot{u_e} = u_{0e} - u_e - \beta \nu_e - w_{ef}[u_f]^+ - \sum_{j=1}^{j=n} h_j[s_j] \quad (1)$$

$$\tau_2 \dot{\nu_e} = -\nu_e + [u_e]^+ \quad (2)$$

$$\tau_1 \dot{u_f} = u_{0f} - u_f - \beta \nu_f - w_{fe}[u_e]^+ - \sum_{j=1}^{j=n} h_j[s_j]^- \quad (3)$$

J.-K. Ryu is with the Mechanical Engineering R&D Lab., LIG nex1, Gyeonggi 446-506, Korea {upright}@lignex1.com

N.Y. Chong is with the School of Information Science, Japan Advanced Institute of Science and Technology, Ishikawa 923-1292, Japan

B.J. You is with the Center for Cognitive Robotics Research, Korea Institute of Science and Technology, Seoul 136-791, Korea

H. Christensen is with the College of Computing, Georgia Institute of Technology, Atlanta, GA 30332, USA

978-1-4244-5081-7/09/$26.00 ©2009 IEEE

$$\tau_2 \dot{\nu}_f = -\nu_f + [u_f]^+ \quad (4)$$

$$y_i = [u_i]^+ = max(u_i, 0), [u_i]^- = min(u_i, 0) \quad (5)$$

$$y_{out} = [u_e]^+ + [u_f]^+ = y_e - y_f \quad (6)$$

where u_e, ν_e, u_f, and ν_f are the internal states of the oscillator. y_{out} is the output of the oscillator. β, w, and h are the weights of the inter-oscillator and the input signal. s is an external input to the oscillator. τ_1 and τ_2 are the positive time constants that determine the envelope and frequency of the oscillator's output. $u_{0e,0f}$ is the positive tonic input that modulates the output amplitude. To maintain a stable oscillation, we set the time constant ratio to a value falling within the range of 0.1-0.5 [8].

2) Frequency Adaptation Rule: Designing a frequency adaptation rule is very challenging, especially when there is no *a priori* knowledge about the oscillator or its network [15]. In our previous work, we proposed an evolutionary approach for enabling frequency-adaptive behaviors of Matsuoka's neural oscillator based on an evolutionary searching and phase-locking behavior [16]. The difference in phase is tightly locked if the frequency of the input signal is close to that of the limit-cycle system and the amplitude of the input signal is large enough. With such phase-locking effect, we can consider the frequency-adaptive rule of nonlinear oscillators in the phase plane. The frequency adaptation rule was assumed to be a linear combination of local variables in the phase plane, which is dependent on the relation between the input signal and the state of the phase point that rotates along the limit cycle [17]. We choose the frequency-adaptation rule of Matsuoka's neural model as follows:

$$\dot{\tau}_1(t) = -\eta S_{external} \times (w_1 u_e + w_2 \nu_e + w_3 u_f + w_4 \nu_f + w_5 \dot{u}_e + w_6 \dot{\nu}_e + w_7 \dot{u}_f + w_8 \dot{\nu}_f) \quad (7)$$

$$\tau_2(t) = \tau_1(t)/R \quad (8)$$

where $0 < \eta < 1$ is the constant that determines the learning rate. w_1 through w_8 are the weight factors that describe the relation among the variables. The amplitude of the input signal $S_{external}$ is multiplied to affect the frequency adaptation only when the input signal is activated. The minus sign is determined by the rotation direction of the oscillator. R is the pre-determined time constant ratio between τ_1 and τ_2. We encoded only four weight factors (w_1, w_2, w_5, w_6) of the extensor neuron because the extensor neuron and the flexor neuron have mutually inhibitory connections. In the evolution process, we set the parameters of the oscillator as follows: $\tau_{1_{initial}}$=0.3, R=0.5, β=2.5, h=0.6, w_{ef}=w_{fe}=2.5, u_{0e}=u_{0f}=1.0, and η=0.01. The external signal is represented by $S_{external} = sin5t$.

We employed a genetic algorithm (GA) for discovering the relation among the variables of the frequency-adaptive rule. The real-coded GA was implemented as follows: first, the initial population is determined. Then, two individuals are randomly selected to produce offspring fivefold. We used the UNDX crossover and no mutation. After the production, the offspring, called the search space, is evaluated by an objective function. Two best individuals in the offspring

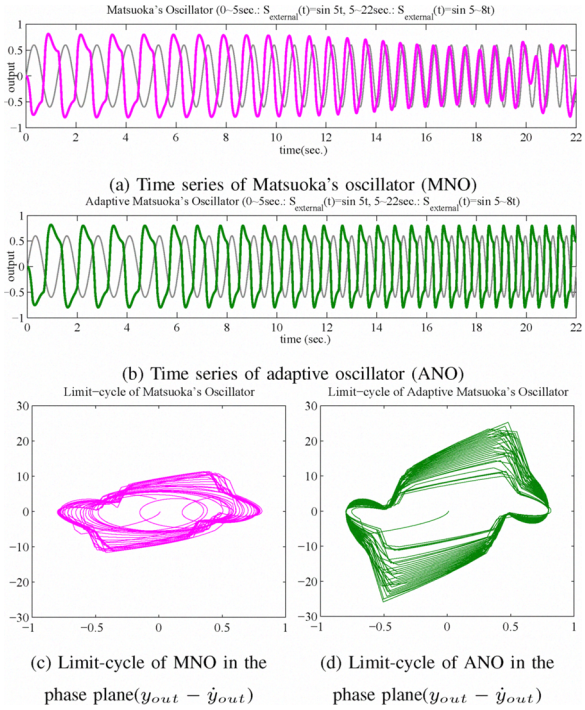

Fig. 1. Frequency adaptation of adaptive oscillator

replace the selected individuals in the population, which is known as the minimal gap generation (MGG) model. This process iterates until the termination condition is satisfied. Each loop of the algorithm is referred to as a generation. Finally, we can obtain an optimal adaptation rule of the oscillator.

3) Entrainment property enhancement: Now we verify the frequency adaptation capability of the proposed oscillator to a varying input signal as shown in Fig. 1. The sinusoidal input signal's frequency, at 5 sec., increases gradually from 5 Hz to 8 Hz as time goes. The frequency-adaptive oscillator remarkably entrains to the varying input signal keeping a specific phase difference. This result is encouraging. Therefore, once the parameters (or the weighting factors of the frequency adaptation rule) have been tuned, we can have the CPG cope with a wider range of external uncertainties and changes in real time and obtain the appropriate parameter values for a desired periodic signal. To investigate the convergence and the entrainment capability of the frequency-adaptive oscillator, we performed simulations with various input signals. Fig. 2 shows the adaptation of the proposed oscillator to the input signals of various types.

III. NEURAL CONTROLLER FOR A ROBOTIC LEG

We apply the frequency-adaptive Matsuoka's neural oscillator to build an adaptive controller for a robotic leg. The controller consists of the adaptive CPG for the trajectory generation and the coordination of healthy and robotic legs with impact absorption as shown in Fig. 3. Sensory feedbacks such as a touch signal and articulation angles from the healthy leg are connected directly to the adaptive CPG of the robotic leg. It allows easy synchronization between both

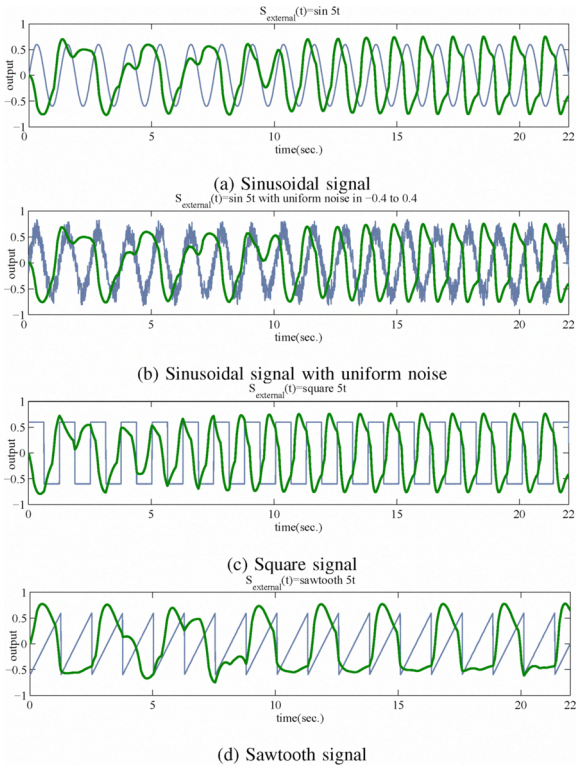

Fig. 2. Frequency adaptation of adaptive oscillator with various signals

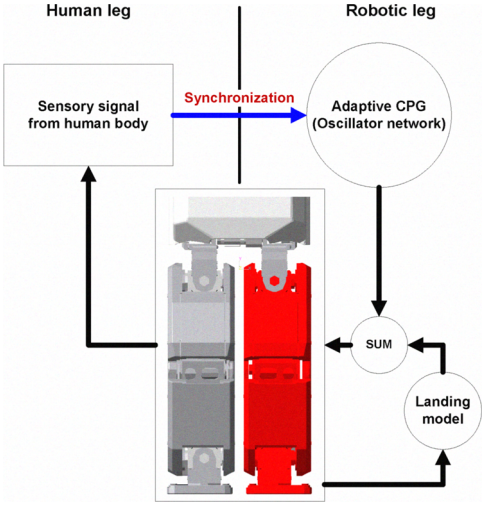

Fig. 3. Control architecture for coordinating healthy and robotic limbs (in red)

legs and provides natural walking motions of the amputee. The spring-damper landing model reduces impacts when the robotic leg touches on the ground since the impact may cause a fracture and uncomfortable wearing feeling.

A. Adaptive Central Pattern Generator

We construct the adaptive CPG that is a network of neural oscillators with frequency adaptation capability, which can produce an arbitrary rhythmic patterns for each joint and keep the rhythmic pattern with a specific phase lag according to the input signal's frequency variation by self-modulating

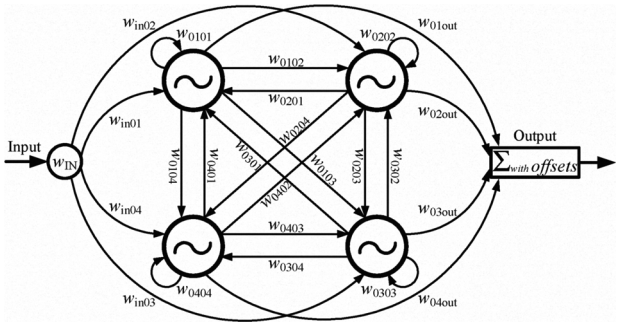

Fig. 4. Structure of neural oscillator network (NON)

the frequency of the CPG.

1) Neural Oscillator Network (NON) Module: Now, we propose a multi-number neural oscillator system for controlling each DOF of the robotic leg by generating multidimensional trajectories (that a single oscillator may not be able to produce). Our basic idea is to construct a network of 4 oscillators through appropriate connection weights for each DOF, so that the network can generate arbitrary rhythmic signals as illustrated in Fig. 4. Each neural oscillator has the same internal parameters in order to simplify the incorporation of the feedback pathway into the network and the coupling process with other modules in the network. We tuned the connection weights between the oscillators and the offset of each oscillator's output using an evolutionary computation approach: $(\mu/\mu_W, \lambda)$-CMA-ES (Evolution Strategy with Covariance Matrix Adaptation) [20], enabling the generation of desired motion trajectories for each DOF. We use a distributed memory massively parallel MIMD supercomputer designed by Cray Inc. for computing the fitness of each individual. Since the evaluation of each individual requires the simulation of oscillator network module, distributed computation dramatically improved the performance of our evolutionary strategy. We used 60 processors to perform the evaluation of each individual and tune the parameters for constructing the local oscillator network. The evolutionary strategy program was built with MPI library.

2) Adaptive NON module: As previously mentioned, if the input signal frequency is far away from the oscillator's intrinsic frequency, the synchronization between those two frequencies will not occur. Moreover, the oscillator's output pattern will not be maintained. Therefore, the oscillator network module cannot keep its motion trajectory (that has been tuned by the evolutionary computation strategy) to be well suited to variations of the frequency difference between the module's intrinsic frequency and the input signal. To cope with this problem, we incorporate the frequency adaptation rule given in Eqn. 7 with the NON module into the CPG. It not only enhances the entrainment capability, but also keeps its desired pattern of the module according to changes in the input signal's frequency. To investigate properties of the adaptive oscillator network module as a CPG, we performed numerical simulations with various input signal and initial values as shown in Fig. 5. Fig. 5-(a) shows a target pattern

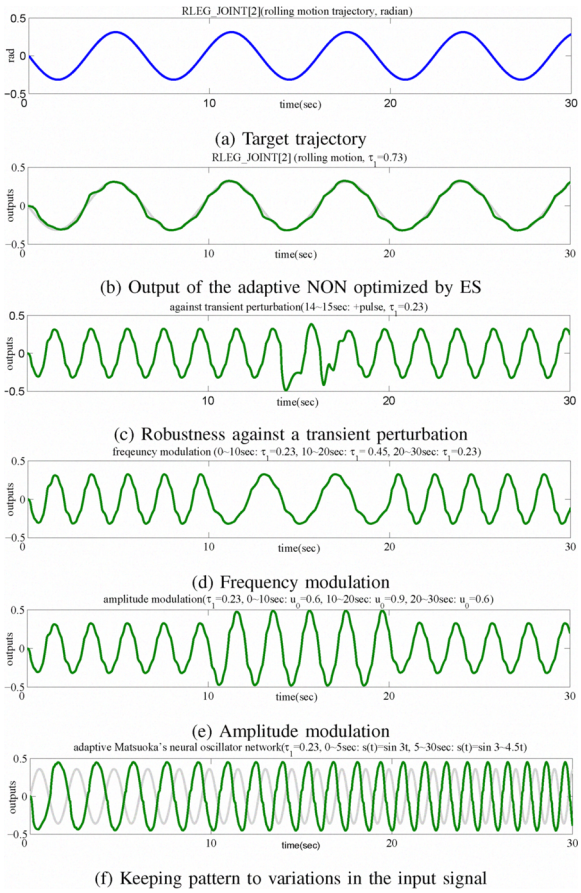

Fig. 5. Properties of the adaptive NON

for rolling motion of RLEG_JOINT[2] of HOAP-3. Fig. 5-(b) is the output of the adaptive NON module optimized by the evolutionary strategy. The adaptive CPG module's output frequency and amplitude can be easily modulated by controlling some parameters. It has robustness against transient perturbations because of its limit-cycle property, which can keep its intrinsic pattern as the input signal varies in frequency (see Fig. 5-(c, d, e, f)).

3) Structure of adaptive CPG for a biped: We particularly focus on the pitching and rolling motions of each leg, considering only 10 DOFs among 28 DOFs. Fig. 6 shows a schematic view of the humanoid's kinematic configuration and the motion pattern generator. We employ the local oscillator network of 4 oscillators for each DOF as shown in Fig. 4. Each local network functions as a single oscillator since the four oscillators have the same internal parameters yielding the same frequency and amplitude. Note that in human walking, the legs and arms on the same side swing in the opposite phase, and the legs and their contralateral arms swing in the same phase. Therefore, in order to synchronize the phase difference of the healthy and robotic legs, we construct a connection to the adaptive CPG from the healthy leg's touch signal. Through the overall network, the adaptive neural oscillator adapts its frequency to the sensory feedback signal (by self-modulating the time constant), and simultaneously transmits the parameter to other local oscillator

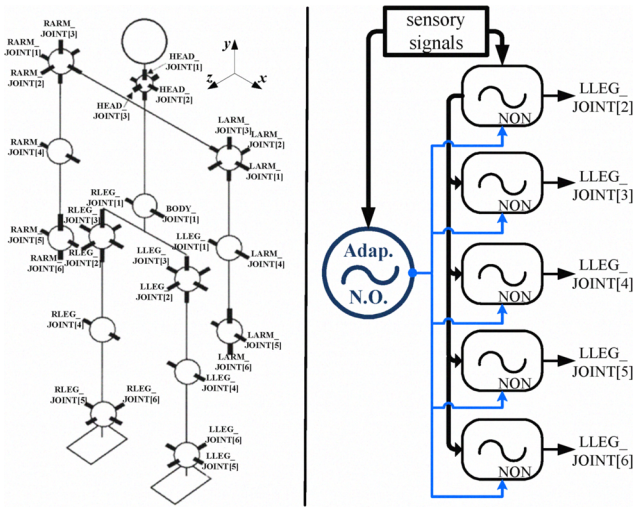

Fig. 6. Schematic view of the proposed CPG for a robotic leg

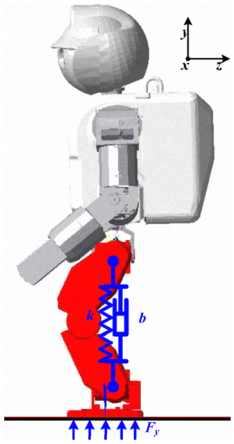

Fig. 7. Landing model for impact absorption

networks, enabling the global entrainment for healthy and robotic legs.

B. Landing Model for Impact Absorption

To secure the stability of locomotion, the robotic leg needs to incorporate sensory feedback from interactions with the ground. Specifically, we attach a spring-damper component between the hip and ankle joints to absorb an impulsive ground reaction force at landing as shown in Fig. 7. Here the equation for interaction with the ground can be described by the following equation.

$$m\frac{d^2y(t)}{dt^2} + b\frac{dy(t)}{dt} + ky(t) \quad = \quad F_y \qquad (9)$$

where $y(t)$ is the displacement of the mass m along the vertical axis, and F_y is the normal ground reaction force on the supporting feet. We control properly the damping factor b and the spring coefficient k of the spring-damper component so that the impact force is minimized. The joint positions according to the displacement $y(t)$ are calculated

TABLE I

PHYSICAL PROPERTIES OF HOAP-3

Link	Weight (kg)	Height (m)
Foot	0.349	0.040
Calf	0.328	0.105
Thigh	0.519	0.105
Hip	0.2687	-
Arm	0.8565	0.281
Upper body	4.16	0.35
Total body	8.8024	0.6

by the following equations.

$$\theta_h^p(t) = \theta_{h\cdot cpg}^p(t) + \theta_{sd}^p(t) \quad (10)$$

$$\theta_k^p(t) = \theta_{k\cdot cpg}^p(t) - 2\theta_{sd}^p(t) \quad (11)$$

$$\theta_a^p(t) = \theta_{a\cdot cpg}^p(t) + \theta_{sd}^p(t) \quad (12)$$

where $\theta_h^p(t)$, $\theta_k^p(t)$, and $\theta_a^p(t)$ are the pitching angles of the hip, knee, and ankle joints, respectively. $\theta_{h\cdot cpg}^p(t)$, $\theta_{k\cdot cpg}^p(t)$, and $\theta_{a\cdot cpg}^p(t)$ are produced by the adaptive central pattern generator. $\theta_{sd}^p(t) = \arcsin(y(t)/L)$ is the joint angle compensation induced by the spring-damper component, and L is the length of the thigh.

IV. SIMULATION RESULTS

We verify the validity of the proposed controller for achieving automatic synchronization between healthy and robotic legs using our in-house locomotion simulator running within the RecurDyn environment, a multi-body dynamic analysis program. Table I shows the physical parameters of the HOAP-3 used in the simulation. The analysis took about 60 sec. for 1 sec. locomotion simulation on a personal computer (Intel Core2 Duo 3.0 GHz).

We investigate whether a robotic leg can adapt its swing frequency to the changes in the swing frequency of a healthy leg. Here the left leg is assumed to be a robotic leg, and the touch signal of the healthy right leg is fed to the adaptive CPG of the robotic leg. The right leg was controlled by preplanned motion trajectories, where the swing frequency increased to 0.17 Hz from 0.13 Hz. Fig. 8 shows that the robotic leg can adequately synchronize its trajectories according to the touch signal of the right leg. Fig. 8-(a) is the reaction force exerted on the right foot which was fed to the CPG. Fig. 8-(b) is the switching period of the center of mass (COM) between the right and left feet. Figs. 8-(c, d, e, f, g) show the trajectories of each joint of the robotic leg. It can be observed that the adaptive CPG generated new but fairly stable trajectories in real-time according to the changes in the right legs's swing frequency after 30 sec. The gray solid lines mean the nominal trajectories generated from the adaptive CPG tuned by the $(\mu/\mu_W, \lambda)$-CMA-ES in advance. The landing model modulates the pitching motion of the robotic leg to absorb the impact force as shown in 8-(d, e, f). Fig. 8-(h) shows the variation of $y(t)$ (see Eqn. 9) when the ground impact force is exerted on the left leg. Through the use of adaptive CPG and landing model, the robotic leg

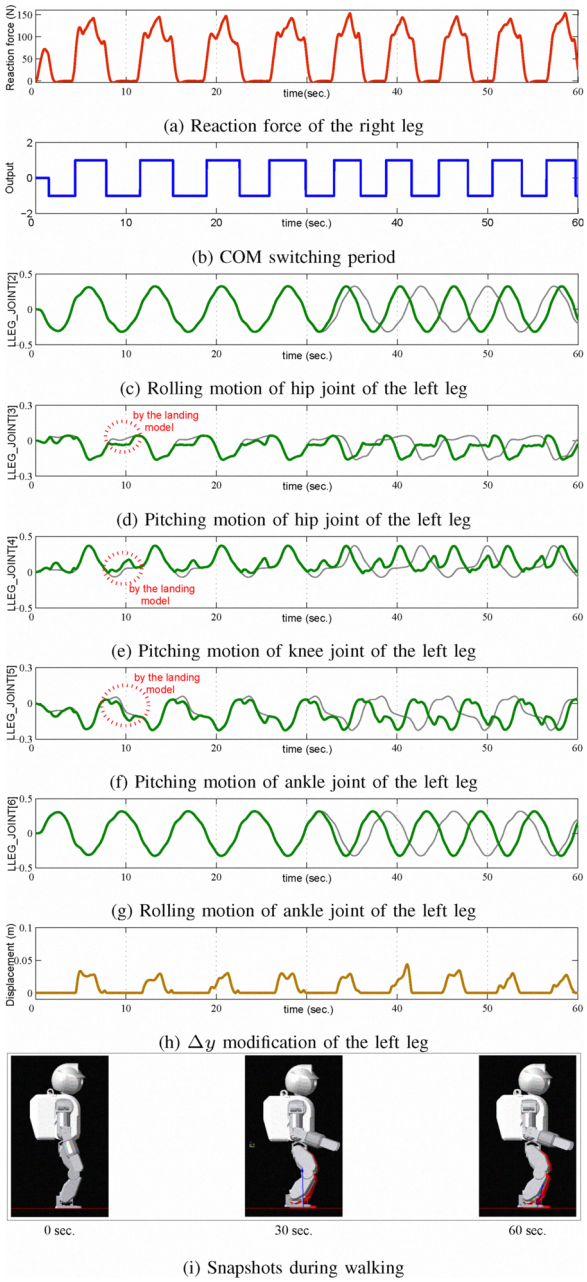

Fig. 8. Joint angle (rad.) of the robotic leg using the right leg's touch signal (The gray lines mean nominal trajectories. At 30 sec., the swing frequency of the right leg changes to 0.17 Hz from 0.13 Hz.)

can naturally keep its swing frequency in accordance with the healthy leg and minimize the ground reaction force.

V. CONCLUSIONS

This paper presented an evolutionary approach to finding the basic rule of a network of nonlinear oscillators for frequency adaptation under variations of rhythmic behavior. It enabled the fast and accurate entrainment of the input signal in a wide variety of ranges and types. Exploiting the frequency adaptation rule, we constructed an adaptive CPG that can produce multidimensional rhythmic trajectories, and adapt its output pattern autonomously to a changing periodicity of the input signal. The adaptive CPG provides

an easy and efficient way to coordinate movements of each individual limb according to the changes in environments, external requirements, or proprioceptive information. We applied the proposed adaptive CPG to the coordinated control of healthy and robotic legs for the purpose of dynamic swing frequency adaptation. In addition, to increase the stability of the prosthesis, a spring-damper component was attached between the hip and ankle joints, allowing the absorption of impulsive ground reaction forces at landing. Through a series of rigorous dynamic simulations with a humanoid robot, our adaptive control architecture has proven very effective in coordinating lower limb movements. Eventually, the proposed approach can be extended to be applied to coordinating the healthy and robotic upper and lower limbs in a natural way. In order to validate the proposed adaptive CPG in real-world test environments, we are currently implementing this approach in a real humanoid robot.

REFERENCES

[1] L. J Marks and J. W Michael, Science, medicine, and the future: artificial limbs, *BMJ*, 323:732-735, 2001.

[2] S. Ferguson and G R. Dunlop, "Grasp recognition from myoelectric signals," *Proc. Australasian Conf. on Robotics and Automation*, 27-29, 2002.

[3] M. C. Carrozza, F. Vecchi, F. Sebastiani, G. Cappiello, S. Roccella, M. Zecca, R. Lazzarini, and P. Dario, "Experimental analysis of an innovative prosthetic hand with proprioceptive sensors," *Proc. IEEE Intl Conf on Robotics and Automation*, 14-19, 2003.

[4] J. Burridge, M. Haugland, B. Larsen, N. Svaneborg, H. Iversen, P. B. Christensen, R. Pickering, and T. Sinkjaer, "Long-term follow-up of patients using the ActiGait implanted drop-foot stimulator," *Annual Conf. of Intl FES Society*, 2005.

[5] G. Taga, Y. Yamaguchi, H. Shimizu, Self-organized control of bipedal locomotion by neural oscillators in unpredictable environment, *Biological Cybernetics*, 65:147-159, 1991.

[6] H. Kimura, K. Sakurama, and S. Akiyama, "Dynamic walking and running of the quadraped using neural oscillators," *Proc IEEE/RSJ Intl Conf on Intellgent Robots and Systems*, 50-57, 1998.

[7] A. J. Ijspeert, J. Hallam, and D. Willshaw, "From lampreys to salamanders: Evolving neural controllers for swimming and walking," *Intl Conf on Simulation of Adaptive Behavior*, 390-399, 1998.

[8] M. Williamson, *Robot arm control exploiting natural dynamics*, PhD thesis, Massachusetts Institute of Technology, Cambridge, MA, 1999.

[9] L. Righetti, J. Buchli, and A. J. Isjpeert, Dynamic hebbian learning in adaptive frequency oscillators, *Physica D*, 216:269-281, 2006.

[10] R. Héliot and B. Espiau, Online generation of cyclic leg trajectories synchronized with sensor measurement, *Robotics and Autonomous Systems*, 56:410-421, 2008.

[11] K. Doya and S. Yoshizawa, Adaptive synchronization of neural and physical oscillators, *Advances in Neural Information Processing Systems*, 4:109-116, 1992.

[12] B. Ermentrout and N. Kopell, Learning of phase lags in coupled oscillators, *Neural Computation*, 6:225-241, 1994.

[13] R. S. Sutton and A. G. Barto, Toward a modern theory of adaptive networks: expectation and prediction, *Psychological Review*, 88(2):135-170, 1981.

[14] J. Nishii, A learning model for oscillatory networks, *Neural Networks*, 11:249-257, 1998.

[15] X. Yao, "Evolving artificial neural networks," *Proc. of the IEEE*, 87(9):1423-1447, 1999.

[16] J. K. Ryu and N. Y. Chong, "An adaptive neural oscillator for swing-up control of the acrobot," *Proc. Int. Conf. on Computational Intelligence, Robotics and Autonomous Systems*, 166-171, 2007.

[17] A. Pikovsky, M. Rosenblum, and J. Kurths, *Synchronization: a universal concept in nonlinear science*, Cambridge University Pres, 2001.

[18] K. Matsuoka, Sustained oscillations generated by mutually inhibiting neurons with adaptation, *Biological Cybernetics*, 52:97-111, 1985.

[19] A. M. Arsenic, "On stability and tuning of neural oscillators: application to rhythmic control of a humanoid robot," *Proc. IEEE Intl Joint Conf on Neural Networks*, 1:99-104, 2004.

[20] N. Hansen and A. Ostermeier, Completely derandomized self-adaptation in evolution strategies, *Evolutionary Computation*, 9(2):159-195, 2003.